Journal of Physiology (1995), 485.2, *pp.* 403–418

Fractional calcium currents through recombinant GluR channels of the NMDA, AMPA and kainate receptor subtypes

N. Burnashev*, Z. Zhou†‡, E. Neher† and B. Sakmann*§

**Max-Planck-Institut für medizinische Forschung, Abteilung Zellphysiologie, 69120 Heidelberg, Germany, †Max-Planck-Institut für biophysikalische Chemie, Abteilung Membranbiophysik, 37077 Göttingen, Germany and ‡Institute of Biophysics and Biochemistry, Huazhong University of Science and Technology, Wuhan, Hubei 430074, China*

1. Simultaneous fluorescence and whole-cell current measurements using the calcium indicator dye fura-2 were made in HEK 293 cells expressing recombinant glutamate receptor (GluR) channels, and fractional Ca^{2+} currents (the proportion of whole-cell current carried by Ca^{2+}; P_f) were determined.

2. Cells expressing *N*-methyl-D-aspartate receptor (NMDAR) channels showed glutamate-activated Ca^{2+} inflow in the voltage range −60 to 40 mV in normal extracellular solution. Ca^{2+} inflow decreased in a voltage-dependent manner at membrane potentials more negative than −30 mV due to Mg^{2+} block. Voltage dependence of block at negative potentials was stronger in cells expressing the NR1–NR2A as compared with cells expressing NR1–NR2C subunits.

3. Fractional Ca^{2+} currents through NMDARs were independent of extracellular Mg^{2+} and varied between 8·2% (NR1–NR2C subunits) and 11% (NR1–NR2A subunits) in normal extracellular solution (1·8 mM Ca^{2+}) at −60 mV membrane potential. P_f values increased with increasing $[Ca^{2+}]_o$ in the range of 0·5–10 mM $[Ca^{2+}]_o$ in a saturating fashion.

4. In cells expressing α-amino-3-hydroxy-5-methyl-4-isoxazolepropionate receptor (AMPAR) subunits which were unedited at the Q/R site of the putative transmembrane segment TM2 (Q-form), or in cells coexpressing unedited and edited subunits (R-form), the glutamate-evoked Ca^{2+} inflow increased from 20 to −80 mV in an almost linear way.

5. Fractional Ca^{2+} currents through AMPAR channels depended on subunit composition. P_f values of Q-form homomeric channels at −60 mV and 1·8 mM $[Ca^{2+}]_o$ were between 3·2 and 3·9%. They were slightly voltage dependent and increased with $[Ca^{2+}]_o$ in the range 1·8–10 mM. P_f values in cells co-expressing Q- and R-form subunits were almost one order of magnitude smaller (0·54%).

6. Relative concentrations of Q-form and R-form GluR-B subunit-specific cDNAs used for cell transfection determined the expression of functionally different heteromeric AMPARs. P_f decreased with increasing relative concentration of R-form encoding cDNAs from 3·4 to 1·4%, demonstrating that editing of the Q/R site of GluR-B subunits decreases Ca^{2+} inflow through heteromeric AMPARs.

7. Cells expressing the GluR-6 subunit of the kainate receptor (KAR) family were characterized by P_f values which depended on the editing in the TM1 and TM2 segments. P_f values were largest for the Q-form (1·55–2·0%) and lowest for R-form channels (< 0·2%), suggesting that Q/R site editing also decreases Ca^{2+} inflow through KAR channels. Cells co-expressing both subunit forms showed an intermediate value (0·58%).

§ To whom correspondence should be addressed.

8. Fractional Ca^{2+} currents measured with normal $[Ca^{2+}]_o$ were different from P_f values predicted with constant field assumptions from reversal potentials measured in bi-ionic (Ca^{2+}–Cs^+) conditions with high $[Ca^{2+}]_o$.
9. The results indicate that the size of P_fs mediated by recombinant GluR channels in normal extracellular solution varies over a 50-fold range between less than 0·2 and 11 %, depending on the combination of GluR channel subunits expressed. Assembly of different subunit combinations, relative abundance of subunit specific mRNAs and editing of mRNA are major mechanisms which control this wide range of Ca^{2+} inflow through different versions of GluR channels under physiological conditions.

Inflow of calcium ions via synaptic glutamate receptor (GluR) channels may be a critical step in controlling developmental changes in synaptic connectivity and plasticity in the central nervous system (CNS) (Collingridge & Bliss, 1987; Nicoll, Kauer & Malenka, 1988; Collingridge & Singer, 1990). Ca^{2+} influx is mediated by the opening of GluR channels which are heterogeneous in their functional properties and molecular structure. They are multimeric proteins assembled from subunits which belong to different subunit families (Wisden & Seeburg, 1993). Based on pharmacological criteria GluRs are referred to as the α-amino-3-hydroxy-5-methyl-4-isoxazolepropionate receptor (AMPAR), *N*-methyl-D-aspartate receptor (NMDAR), and kainate receptor (KAR) channels (Monaghan, Bridges & Cotman, 1989; Watkins, Krogsgaard-Larsen & Honore, 1990). Measurements of bi-ionic reversal potentials of glutamate-activated currents in host cells expressing recombinant GluR channels have suggested that, based on shifts of reversal potential in Ca^{2+}-free and high extracellular Ca^{2+} concentration ($[Ca^{2+}]_o$) solutions, their relative calcium to monovalent alkali cation (M^+) permeability (P_{Ca}/P_M) varies over a wide range, and that P_{Ca}/P_M depends strongly on subunit composition (Hollmann, Hartley & Heinemann, 1991; Burnashev, Monyer, Seeburg & Sakmann, 1992*a*; Burnashev *et al.* 1992*b*; Köhler, Burnashev, Sakmann & Seeburg, 1993; Monyer, Burnashev, Laurie, Sakmann & Seeburg, 1994). In such experiments reversal potentials were measured with unphysiologically high $[Ca^{2+}]_o$ (10–110 mM). To assess the amount of glutamate-activated Ca^{2+} inflow mediated by different GluR channels under more physiological conditions (1·8 mM $[Ca^{2+}]_o$), the contribution of Ca^{2+} to the total current mediated by GluR channels ought to be determined using simultaneous fluorescence and current measurements (Neher & Augustine, 1992; Zhou & Neher, 1993; Schneggenburger, Zhou, Konnerth & Neher, 1993).

We have measured glutamate-activated whole-cell currents in HEK 293 cells expressing recombinant GluRs and determined simultaneously the rise in intracellular Ca^{2+} concentrations ($[Ca^{2+}]_i$) by two-wavelength fura-2 fluorescence measurements under conditions which allow the estimation of a fractional Ca^{2+} current (P_f). The results show that P_fs mediated by different GluR channels with physiological $[Ca^{2+}]_o$ may vary between less than 0·2 and 11 % of the total membrane current, and that this fraction depends critically on their subunit composition.

METHODS

Recombinant glutamate receptor channels in host cells and electrophysiological recordings

Expression of recombinant GluR channels. All measurements were made on HEK 293 cells transfected either transiently or stably with various combinations of cDNAs encoding different subunits of the NMDAR, AMPAR and KAR families. Recordings from transiently transfected cells were made about 2 days after transfection as described by Burnashev *et al.* (1992*a*). Experiments with stably transfected cells (expressing GluR-A subunits) were made 1–2 days after plating.

Electrophysiology and agonist application. Currents were measured in the whole-cell configuration (Hamill, Marty, Neher, Sakmann & Sigworth, 1981) from cells attached to the bottom of a glass coverslip. The intracellular solution, contained in the recording pipette, consisted of (mM): 140 CsCl, 10 Hepes and 1 fura-2 (pH adjusted to 7·2 with CsOH to a total $[Cs^+]$ of 143·5 mM). Normal rat Ringer (NRR) solution was used as extracellular solution containing (mM): 135 NaCl, 5·4 KCl, 1·8 $CaCl_2$, 1 $MgCl_2$, 10 Hepes (pH adjusted to 7·2 with NaOH). In some experiments with NMDAR channels, nominally Mg^{2+}-free NRR was used. For fluorescence calibration experiments the intracellular solution contained (mM): 100 *N*-methyl-D-glucamine (NMG), 10 Hepes and 1 fura-2 (pH adjusted to 7·2, with HCl). Extracellular solution contained (mM): 100 NMG, 10 Hepes and 10 $CaCl_2$ (pH adjusted to 7·2 with HCl). For activation of GluR channels, agonists were applied for 0·3–2 s by means of a Piezo-driven double-barrelled application pipette (Sommer *et al.* 1990). For the activation of NMDAR channels 100 μM glutamate was applied in the continuous presence of 10 μM glycine. For the activation of AMPAR channels 300 μM glutamate was applied alone or in the presence of 10 μM cyclothiazide to prolong the duration of the non-desensitizing current component. In experiments with KAR channels 50 μM of domoic acid (DA) instead of glutamate was used or cells were preincubated with concanavalin A (ConA) at 0·3 mg ml^{-1} for 2–3 min prior to glutamate (300 μM) applications. All pharmacological agents were purchased from Sigma; fura-2 was obtained from Molecular Probes (Eugene, OR, USA).

Shifts of reversal potential (V_{rev}) were measured by changing from symmetrical Cs^+–Cs^+ (extracellular–intracellular) solutions to bi-ionic Ca^{2+}–Cs^+ conditions. The ion composition of the intracellular solution was similar to that used for P_f measurements,

containing (mM): 143·5 CsCl, 10 Hepes and 5 EGTA (pH adjusted to 7·2 with CsOH). The extracellular solutions were (mM): 143·5 CsCl, or 100 $CaCl_2$, 10 Hepes (pH adjusted to 7·2 with CsOH or $Ca(OH)_2$; the final $[Ca^{2+}]$ was 102 mM). The reference electrode in the bath was an agar bridge saturated with 3 M KCl connected to the amplifier via a chlorided silver wire. The shift in junction potential, when switching the extracellular solution from 143·5 mM CsCl to 102 mM $CaCl_2$ was 9·3 mV as measured by a blunt patch pipette filled with 3 M KCl. The measured shift in zero current potential between Cs^+–Cs^+ and Ca^{2+}–Cs^+ conditions was corrected by the junction potential. Zero current potentials were determined by interpolation of the I–V relation of glutamate-activated currents which were measured with 5 or 10 mV steps in holding potential.

Fluorescence measurements

Fura-2 was loaded into HEK 293 cells via the patch pipette and the fluorescence, excited alternately at 360 and 380 nm by means of a rotating filter wheel, was sampled at 2 Hz. Fluorescence was measured by the method described by Schneggenburger *et al.* (1993) and Zhou & Neher (1993) using the photomultiplier and analysis system of Luigs and Neumann (Ratingen, Germany). The Ca^{2+} influx was estimated from the fluorescence signals according to the method of Neher & Augustine (1992) and Zhou & Neher (1993). The ratio, f, of the decrement in fluorescence F_{380} (at 380 nm excitation) and the integral (Q) of the glutamate-evoked current during short applications of glutamate was measured as detailed in Fig. 3. The fluorescence amplitude was normalized by using 'standard beads' measured on the same experimental day; 1 bead unit (BU) represented the mean amplitude of F_{380} signals of five to ten standard beads (Zhou & Neher, 1993).

Simulation of constant field behaviour

Voltage dependence of fractional Ca^{2+} current. The P_f values at various membrane potentials expected from constant field assumptions were compared with the experimental data according to:

$$P_f = 1/\{1 + (P_M/P_{Ca})([M^+]/[Ca^{2+}]_o)(1 - \exp(2V_m/\Phi))/4\}, \quad (1)$$

with the permeability ratio P_{Ca}/P_M determined for P_f measured at −60 mV membrane potential and 1·8 mM external Ca^{2+}. $[M^+]$ is total extracellular (or total intracellular) monovalent cation concentration, $[Ca^{2+}]_o$ is external Ca^{2+} concentration, V_m is membrane potential and $\Phi = RT/F = 25{\cdot}42$ mV (at room temperature), where F, R and T are standard thermodynamic parameters. $[M^+]$ and $[Ca^{2+}]$ were corrected for activities as detailed below.

Fractional Ca^{2+} current in physiological solution and relative Ca^{2+} permeability. The relation between P_f and either $[Ca^{2+}]_o$ or bi-ionic reversal potentials (V_{rev}) predicted on the basis of constant field assumptions was calculated according to eqn (1). Room temperature, T, was taken as 295 K, and both extracellular $Na^+ + K^+$ and intracellular Cs^+ (i.e. the total monovalent cations $[M^+]$) were taken as 143·5 mM. For all calculations $[M^+]$ and $[Ca^{2+}]$ were corrected for activities. The activity coefficient for monovalent ions was 0·72 (as for Cs^+). The activity coefficient for 1·8 mM Ca^{2+} (as $CaCl_2$) was 0·57. The permeability ratio P_{Ca}/P_M was calculated from bi-ionic reversal potentials according to the constant field equation (Iino, Ozawa & Tsuzuki, 1990) as:

$$P_{Ca}/P_M = ([M^+]_i/[Ca^{2+}]_o)\exp(V_{rev}/\Phi)(\exp(V_{rev}/\Phi) + 1)/4, \quad (2)$$

where Φ and $[Ca^{2+}]_o$ have the same meaning as in eqn (1), $[M^+]_i$ is the intracellular monovalent cation concentration, V_{rev} is the bi-ionic reversal potential in high (102 mM) Ca^{2+} extracellular solution. In bi-ionic conditions the solutions contained 102 mM Ca^{2+} on the outer and 143·5 mM Cs^+ on the inner side of the membrane. Activity coefficients were 0·52 for 102 mM Ca^{2+}, 0·57 for 1·8 mM Ca^{2+} and 0·72 for 143·5 mM Cs^+. The permeability ratios P_{Ca}/P_M obtained from this equation were used to calculate the expected P_f values in normal extracellular solution (1·8 mM Ca^{2+}) at −60 mV membrane potential by using eqn (1).

RESULTS

Measurement of calcium inflow activated by glutamate in transfected HEK 293 cells

Loading of HEK 293 cells with fura-2

To measure P_fs we used a modification of the method of Neher & Augustine (1992) and Zhou & Neher (1993). Transfected HEK 293 cells were loaded with the indicator dye fura-2 [1 mM] in the recording pipette. During loading the concentration of fura-2 in the cell slowly rose. When fura-2 was in excess of the 'endogenous' Ca^{2+} buffer then, for Ca^{2+} entering from the extracellular side, a stable relation between the decrease in the Ca^{2+}-sensitive fluorescence at 380 nm (ΔF_{380}) and the underlying Ca^{2+} inflow could be observed. To establish a quantitative relation between fluorescence decrement and the Ca^{2+} flux in HEK 293 cells we calibrated the experimental set-up by measuring the fluorescence decrement in a fully loaded cell under conditions where inward current was carried by Ca^{2+} only. In the method of Zhou & Neher (1993) this is achieved by studying currents through Ca^{2+}-specific voltage-activated channels. Since in HEK 293 cells endogenous voltage-activated Ca^{2+} channels are expressed at a very low density (Sun *et al.* 1994) we used a different method for this calibration. HEK 293 cells that express the Ca^{2+}-permeable GluR-A homomeric channel (Burnashev *et al.* 1992*a*) were used and the impermeant cation NMG was present at 100 mM as the major cation both inside and outside of the cell. The only permeant ion on the extracellular side was Ca^{2+} at 10 mM. After establishing whole-cell recording (with a pipette containing 1 mM fura-2), the dye concentration slowly equilibrated with the cell interior as measured by an increase in the Ca^{2+}-insensitive fluorescence signal at 360 nm (Fig. 1*A*, upper trace). At various intervals after the beginning of the loading the extracellular solution was switched briefly to a solution containing 300 μM glutamate to activate GluR-A channels. The resulting influx of Ca^{2+} was measured as a fluorescence decrease at 380 nm (Fig. 1*A*, middle trace) and the increase in $[Ca^{2+}]_i$ was calculated from the fluorescence ratio according to Grynkiewicz, Poenie & Tsien (1985) (Fig. 1*A*, lower trace).

Determination of the F/Q ratio

The increasing proportion of Ca^{2+} bound by fura-2 at two different times of loading is illustrated in Fig. 1*B*. In the

two panels, for practically identical inward currents evoked by glutamate application and carried by Ca^{2+}, the decrease in fluorescence at 380 nm was about twice as large for the second pulse. The ratio of the fluorescence decrement at 380 nm to the current integral (called the F/Q ratio or f) was correspondingly larger for the second glutamate application. The change in $[Ca^{2+}]_i$ on the other hand was much smaller (Fig. 1*B*, upper traces) because of the larger Ca^{2+} buffering capacity of the fura-2-loaded cell. By plotting the F/Q ratio as a function of the Ca^{2+} buffering capacity (κ'_B) of fura-2 (calculated as $\kappa'_B = \Delta[BCa]/\Delta[Ca^{2+}]_i$, according to eqns (30) and (31) in Neher & Augustine, 1992; where [BCa] is the total concentration of Ca^{2+} bound to buffer) an asymptotic value of f, called f_{max}, was reached (Fig. 1*C*) and f_{max} may then be taken as the F/Q ratio representing pure Ca^{2+} flow. The fraction of the whole-cell current carried by Ca^{2+} in multi-ionic conditions is then measured as $P_f = f/f_{max}$. For all measurements the cellular fluorescence values were normalized with respect to the fluorescence of standard fluorescence beads such that fluorescence is expressed as bead units (BU). One bead unit is the fluorescence of a single bead under the illumination condition and fluorescence detection efficiencies of the given experiment. The F/Q ratio has the dimension of bead units

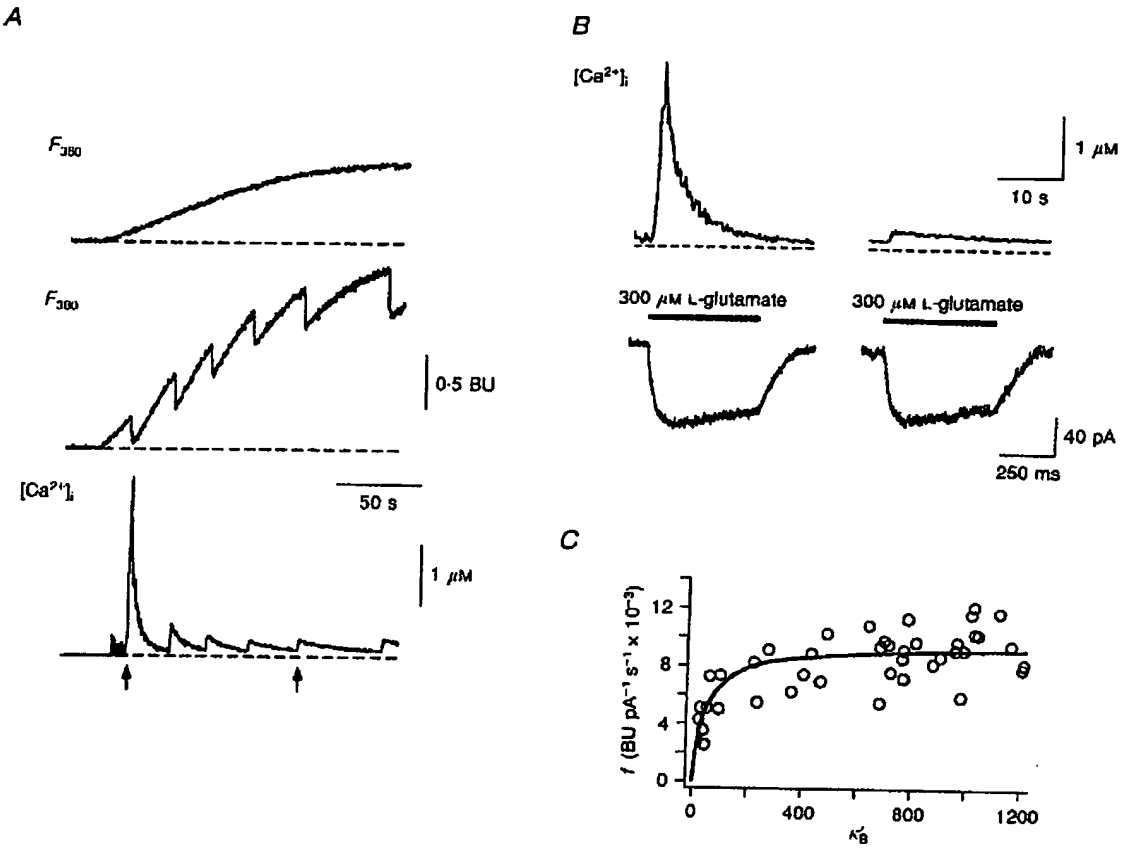

Figure 1. Loading of HEK cell with fura-2, measurement of glutamate-activated $[Ca^{2+}]_i$ changes and saturation of F/Q ratio

For calibration of the fluorescence signal (ΔF) and the Ca^{2+} influx, stably transfected HEK 293 cells were used which expressed the GluR-A subunit homomeric channel. In intracellular and extracellular solutions, Ca^{2+} was the only permeable ion. *A*, fluorescence signals during fura-2 loading (1 mM in the pipette) at 360 nm (upper trace, Ca^{2+}-insensitive fluorescence, indicating degree of loading with indicator dye); at 380 nm (middle trace, indicating fluorescence decrease, ΔF_{380}, upon rise in $[Ca^{2+}]_i$) and ratiometric determination of $[Ca^{2+}]_i$ (lower trace). Loading of cell in NMG (100 mM) extracellular solution containing 10 mM Ca^{2+}. Intracellular solution contained 100 mM NMG. Several pulses of glutamate (300 μM) were applied during loading. *B*, simultaneous measurement of $[Ca^{2+}]_i$ by ratiometric determination (upper traces) and whole-cell Ca^{2+} current (lower traces) during loading of the same cell as shown in *A* to demonstrate that the same size Ca^{2+} current evoked by glutamate applications marked by arrows in *A* evokes progressively smaller $[Ca^{2+}]_i$ signals, as fura-2 dominates buffer capacity of the cell. *C*, saturation of F/Q ratio, f (in bead units (BU) pA^{-1} s^{-1}) is plotted as a function of the Ca^{2+}-binding capacity of fura-2 (κ'_B). Saturation of f with increasing κ'_B is observed after a few minutes of establishing the whole-cell recording configuration, yielding an f_{max} value of $9{\cdot}5 \times 10^{-3}$ BU pA^{-1} s^{-1}. Data points are pooled from 8 cells. Line represents a binding isotherm fitted to data points.

per coulomb and P_f is a dimensionless quantity (Zhou & Neher, 1993).

Calcium inflow through NMDAR channels

Voltage, Mg^{2+} and subunit dependence of Ca^{2+} influx

Native NMDA receptor channels are characterized by a high relative Ca^{2+} permeability and sensitivity to voltage-dependent block by extracellular Mg^{2+} (Mayer, Westbrook & Guthrie, 1984; Mayer & Westbrook, 1987; Ascher & Nowak, 1988). Functional recombinant NMDAR channels may assemble from different subunit combinations, usually comprising NR1 subunits (Moriyoshi, Masu, Ishii, Shigemoto, Mizuno & Nakanishi, 1991) in combination with one or more subunits of the NR2-subunit family

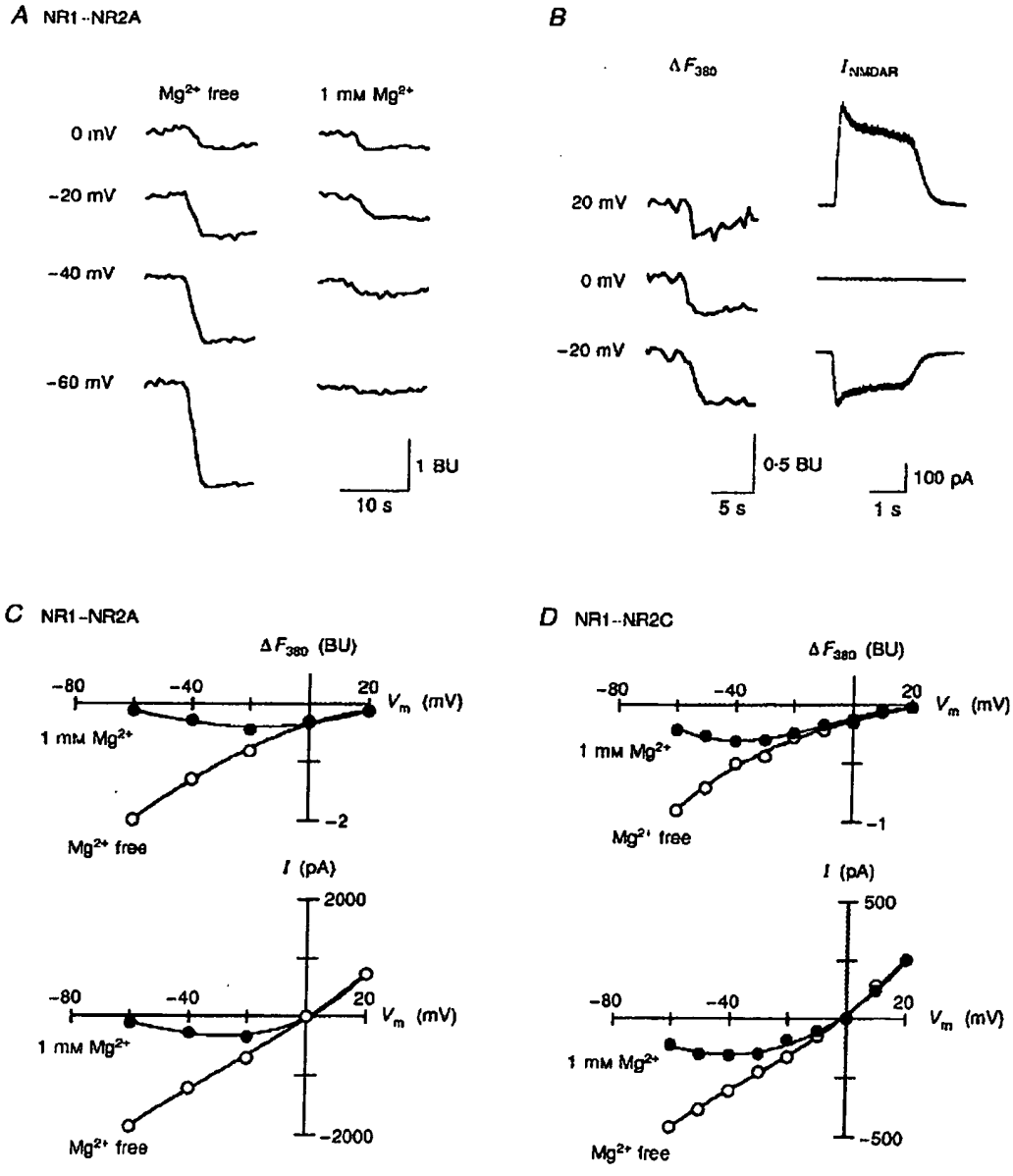

Figure 2. Ca^{2+} influx during activation of NMDAR channels

A, fluorescence decrements (ΔF_{380}) evoked by glutamate application at different membrane potentials (V_m) in the absence (left column) and presence (right column) of extracellular Mg^{2+}. The cell expressed the NR1–NR2A subunit combination. *B*, fluorescence decrements (ΔF_{380}, left) and glutamate-activated currents (I_{NMDAR}, right) close to reversal potential. At −20, 0 and 20 mV a fluorescence decrement is seen, indicating Ca^{2+} inflow even when net current is reversing direction. *C*, fluorescence–voltage (upper graph) and current–voltage (lower graph) plots of a cell expressing the NR1–NR2A subunit combination measured in the absence (○) and presence (●) of extracellular Mg^{2+} (1 mM). *D*, fluorescence–voltage (upper graph) and current–voltage (lower graph) plots of a cell expressing the NR1–NR2C subunit combination measured in the absence (○) and presence (●) of Mg^{2+} (1 mM).

(Monyer *et al.* 1994). Four different combinations of recombinant subunits have a high Ca^{2+} permeability and show clear differences in their sensitivity to Mg^{2+} block (Monyer *et al.* 1994). To evaluate whether NMDAR subtypes show differences in the magnitude and voltage dependence of Ca^{2+} inflow in physiological conditions we measured fluorescence decrements at different membrane potentials in the absence and presence of extracellular Mg^{2+} for cells expressing NR1–NR2A or NR1–NR2C subunits. In all experiments, intracellular [fura-2] was high enough to capture all of the Ca^{2+} entering the cell such that the fluorescence decrement at 380 nm (ΔF_{380}) was proportional to Ca^{2+} influx.

Fig. 2*A*, *C* and *D* illustrates that ΔF_{380} in the absence of extracellular Mg^{2+} rose almost linearly as the membrane potential was made more negative and was reduced in amplitude in the presence of 1 mM Mg^{2+} in a voltage- and subunit-specific manner. Both NMDAR subunit combinations mediated a measurable Ca^{2+} influx at 0 and 20 mV membrane potential in physiological extracellular solution when the glutamate-evoked net current was zero or outwardly directed (Fig. 2*B*–*D*). Recombinant NR1–NR2A

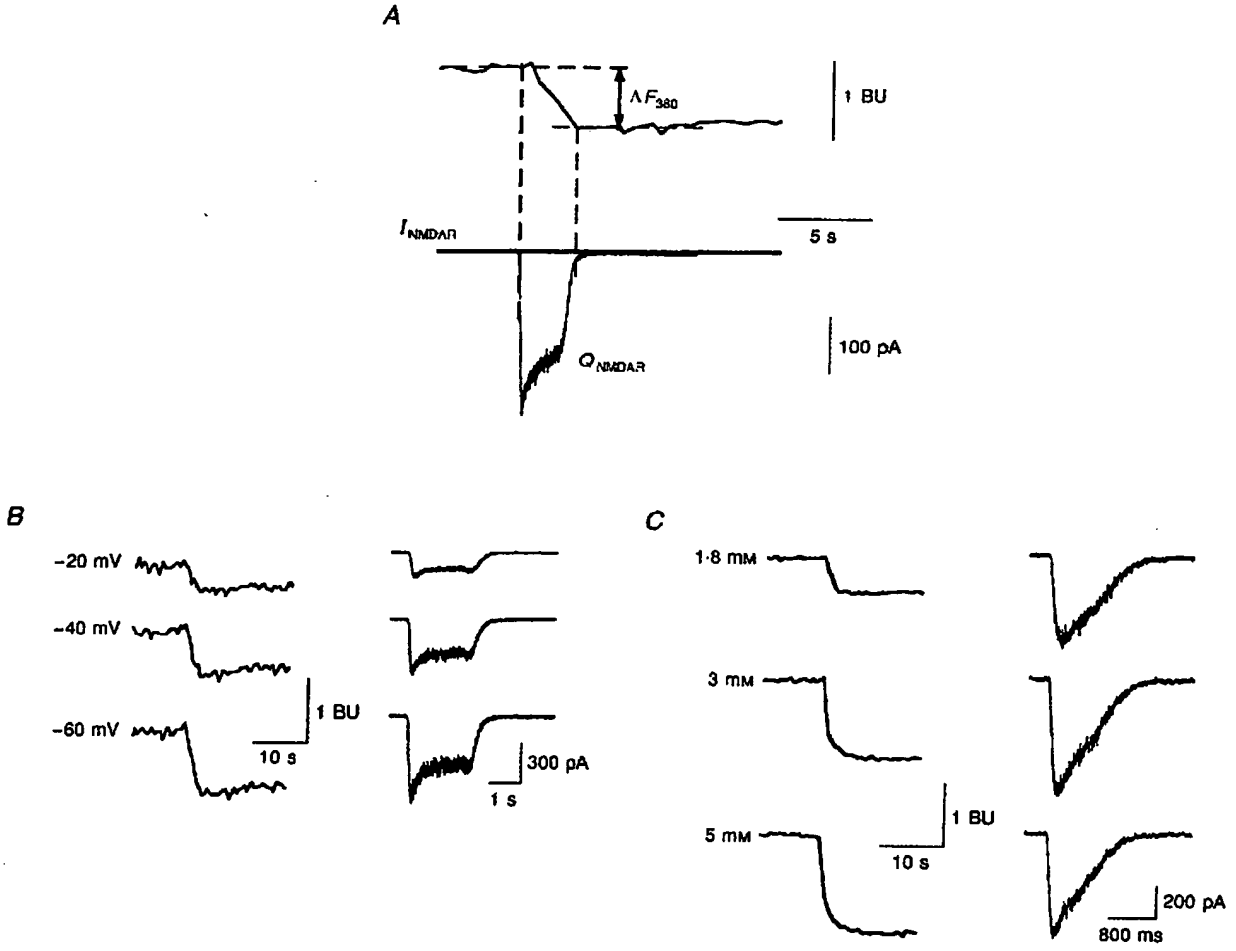

Figure 3. Ca^{2+} influx through NMDAR channels depends on membrane potential and extracellular [Ca^{2+}]

A, determination of *F*/*Q* ratio for recombinant NMDAR channels. Upper trace shows fluorescence decrement (ΔF_{380}) during glutamate application to a cell expressing NR1–NR2A subunits. Arrows indicate amplitude of fluorescence change. Lower trace shows glutamate-activated inwardly directed whole-cell current (I_{NMDAR}). Current integral between dashed lines corresponds to charge transported by the whole-cell current (Q_{NMDAR}). *B*, simultaneous measurement of fluorescence decrement (ΔF_{380}, left column) and glutamate-activated whole-cell currents (I_{NMDAR}, right column) in a cell expressing NR1–NR2A subunits, at different membrane potentials as indicated on the left. Mg^{2+}-free, 1·8 mM Ca^{2+} extracellular solution. Both ΔF_{380} and I_{NMDAR} increase at more negative membrane potentials. *C*, simultaneous measurement of fluorescence decrement (ΔF_{380}, left column) and glutamate-activated whole-cell currents (I_{NMDAR}, right column) at different $[Ca^{2+}]_o$ as indicated on the left. Membrane potential, −60 mV. Cell expressed NR1–NR2A subunit combination. Note that ΔF_{380} increases with $[Ca^{2+}]_o$ for approximately the same I_{NMDAR}.

channels mediated, in physiological extracellular solution (1 mM Mg^{2+}), the largest Ca^{2+} inflow at about −20 mV whereas for NR1–NR2C channels, the largest influx occurred at around −40 mV. The decrease of the fluorescence signal at more negative potentials was much stronger for NR1–NR2A channels compared with that of NR1–NR2C channels.

Fractional Ca^{2+} current through NMDAR channels

To determine the relative contribution of Ca^{2+} to the total current through NMDAR channels, we measured the F/Q ratio (f_{NMDAR}), i.e. the ratio of the fluorescence decrement (ΔF_{380}) to the total charge (Q_{NMDAR}) transported by glutamate-activated current (I_{NMDAR}) during an appropriately selected time interval following NMDAR channel activation (Fig. 3*A*). By dividing f_{NMDAR} by f_{max} the ratio f_{NMDAR}/f_{max} of 11% was obtained for NR1–NR2A recombinant channels at −60 mV. This ratio is equivalent to P_f, the ratio of Ca^{2+} current (I_{Ca}) to the total current (I_{NMDAR}) (Zhou & Neher, 1993). As pointed out by Schneggenburger *et al.* (1993) the F/Q ratio reflects the P_f only if evaluated in relatively short time intervals (within seconds) following Ca^{2+} inflow because for longer times Ca^{2+} clearance will influence the Ca^{2+} balance.

Dependence of fractional Ca^{2+} current on V_m and $[Ca^{2+}]_o$ for two NMDAR channel subtypes

Figure 3*B* illustrates fluorescence (left) and current (right) traces recorded simultaneously during glutamate activation of cells expressing NR1–NR2A subunits in the absence of extracellular Mg^{2+}. As the membrane potential became more negative, both ΔF_{380} and I_{NMDAR} increased. The P_f was almost constant for membrane potentials more negative than −20 mV (Fig. 4*A*) as is expected from constant field assumptions. P_f values showed, over the whole voltage range measured, a clear difference between the two NMDAR channel types, since mean P_f values measured in NR1–NR2A-expressing cells were about 30% larger than those of cells expressing NR1–NR2C subunits (Fig. 4*A*).

The difference in P_f values and bi-ionic (Ca^{2+}–Cs^+) reversal potentials (see Table 1 in Discussion) for two NMDAR subunit combinations might be related to the observation that Ca^{2+} in both types of channels acts as a permeant blocker but of different blocking strength. In cells expressing NR1–NR2A channels, 1·8 mM Ca^{2+} added to divalent-free NRR reduced the whole-cell (inward) current by 23 ± 9% ($n = 6$, $V_m = -60$ mV), whereas for NR1–NR2C channels, the reduction was much larger (50 ± 10%, $n = 5$). In addition, the ratio of chord conductances g_{Ca}/g_{Na}, estimated at −60 mV from the I–V relations measured in 110 mM Ca^{2+} and 140 mM Na^+, respectively, was smaller for NR1–NR2C channels (0·2 ± 0·02, $n = 4$) than for NR1–NR2A channels (0·4 ± 0·08, $n = 5$).

The dependence of P_f on $[Mg^{2+}]_o$ was determined by comparing measurements at 0 and 1 mM Mg^{2+}. The mean P_f values for NR1–NR2A subunit channels at −40 mV of 11·1 ± 0·4% and 11·3 ± 1% ($n = 3$ for each type of experiment), respectively, were not significantly different in spite of the fact that the absolute magnitude of currents in the presence of extracellular Mg^{2+} was much smaller.

Figure 3*C* (left column of traces) illustrates the increase in fluorescence changes evoked by glutamate with increasing $[Ca^{2+}]_o$. The total charge transported by whole-cell currents was of approximately the same magnitude (right column of traces). As expected, P_f values increased with $[Ca^{2+}]_o$. The

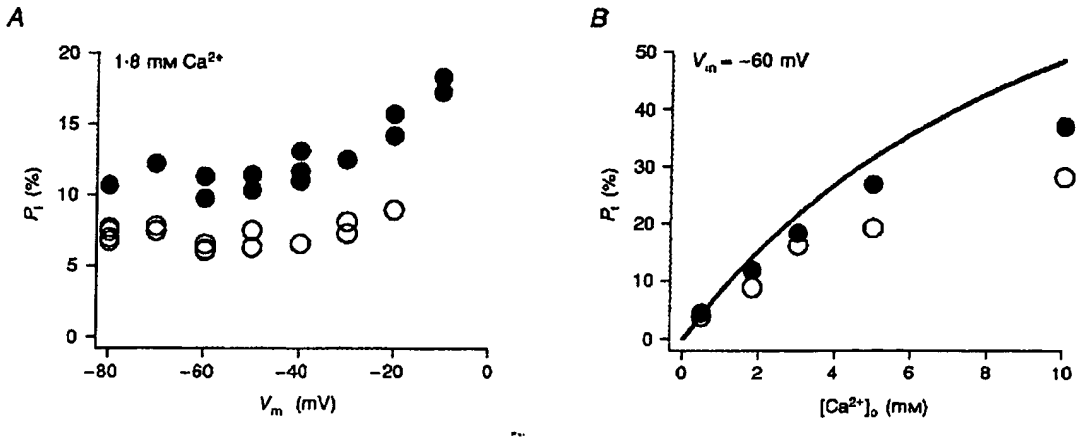

Figure 4. Differences in fractional Ca^{2+} currents between NMDAR channel subtypes

A, voltage dependence of fractional Ca^{2+} currents (P_fs) measured in cells expressing the NR1–NR2A (●) or NR1–NR2C subunit combination (○). Cell transfection as well as P_f measurements were made on the same day for the two subunit combinations. *B*, $[Ca^{2+}]_o$ dependence of P_fs in cells expressing the NR1–NR2A (●) or NR1 NR2C subunit combination (○). Data points represent the mean values from 3–10 cells. For all points the S.D. is within the size of the symbol. Continuous line represents a theoretical curve for P_f–$[Ca^{2+}]_o$ relation for NR1–NR2A channels estimated on the basis of constant field assumptions as detailed in Methods.

P_f *versus* $[Ca^{2+}]_o$ relation tends to saturate at lower values for NR1–NR2C subunit channels than for NR1–NR2A channels (Fig. 4*B*).

Calcium influx through AMPAR channel subtypes

The bi-ionic Ca^{2+}–Cs^+ reversal potential of heteromeric GluR channels of the AMPAR subtype depends critically on the co-assembly of unedited (Q-form) subunits with the edited (R-form) version of the GluR-B subunit (Burnashev *et al.* 1992*a*). Channels formed from different subunit combinations show a high relative Ca^{2+} permeability if the GluR-B subunit is absent or if this subunit is present in the unedited (i.e. GluR-B(Q)) form. We investigated first the Ca^{2+} influx and the P_f of homomeric GluR channels in the Q-form and then determined the effect of GluR-B(R) subunit co-expression.

Voltage dependence of Ca^{2+} influx in Q-form subunit channels

Figure 5*A* illustrates Ca^{2+} inflow measured by ΔF_{380} and the total current I_{AMPAR} at different membrane potentials in a cell expressing GluR-A channels. Ca^{2+} inflow increased almost linearly between 20 and −60 mV. At 0 mV membrane potential, where no net I_{AMPAR} was measurable, an inflow of Ca^{2+} was observed. Also, at positive membrane potentials when the net current was outwardly directed, the inflow of Ca^{2+} could be detected (Fig. 5*B* and *C*).

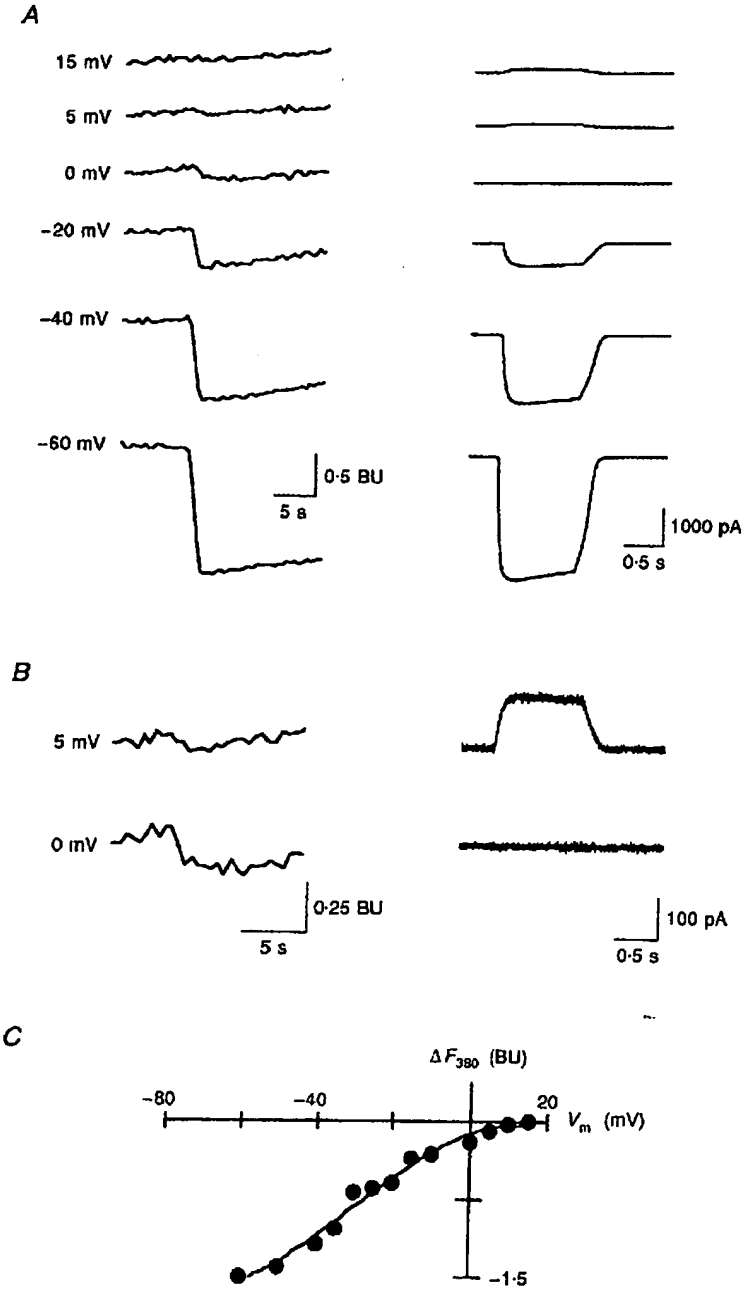

Figure 5. Ca^{2+} flux during activation of homomeric AMPAR channels

A, fluorescence decrement (ΔF_{380}, left) and whole-cell current (I_{AMPAR}, right) measured in normal extracellular solution at different membrane potentials in a cell expressing GluR-A subunits. *B*, illustration at expanded scale of Ca^{2+} inflow measured by ΔF_{380} at 0 and 5 mV membrane potential where no net whole-cell current is detectable (0 mV) or when the current is in the outward direction (5 mV). *C*, voltage dependence of fluorescence decrement (ΔF_{380}) evoked by glutamate in cell expressing homomeric GluR-A channels. Same experiment as shown in *A*.

Similar results were obtained in cells expressing GluR-D homomeric channels.

Fractional Ca^{2+} currents through Q-form subunit channels

To relate Ca^{2+} inflow to the net I_{AMPAR}, we measured P_f by determining the F/Q ratio in the same way as for NMDAR-mediated currents. Figure 6*A* illustrates ΔF_{380} traces and I_{AMPAR} at two membrane potentials and at two $[Ca^{2+}]_o$ for a cell expressing GluR-A subunits.

At −60 mV, P_fs mediated by GluR-A or by GluR-D channels were 3·2 and 3·9%, respectively, and somewhat larger (4·7 and 6%) at −30 mV. P_f values increased at membrane potentials more positive than −30 mV for both subunit channels as expected from constant field assumptions (Fig. 6*B*). The experimental P_f values, however, showed a stronger rectification than predicted. This P_f rectification is opposite to I_{AMPAR} rectification (Burnashev *et al.* 1992*a*), and could be related to the earlier observation that addition of extracellular Ca^{2+} increases the whole-cell Na^+ current at membrane potentials between 0 and −30 mV and blocks the Na^+ current at potentials negative to −30 mV (Burnashev *et al.* 1992*a*). The dependence of P_f on $[Ca^{2+}]_o$, shown in Fig. 6*C* for GluR-A homomeric channels at −30 and −60 mV membrane potential, indicates that in the concentration range tested P_f is considerably smaller than expected for constant field behaviour and the voltage dependence of P_f is independent of $[Ca^{2+}]_o$.

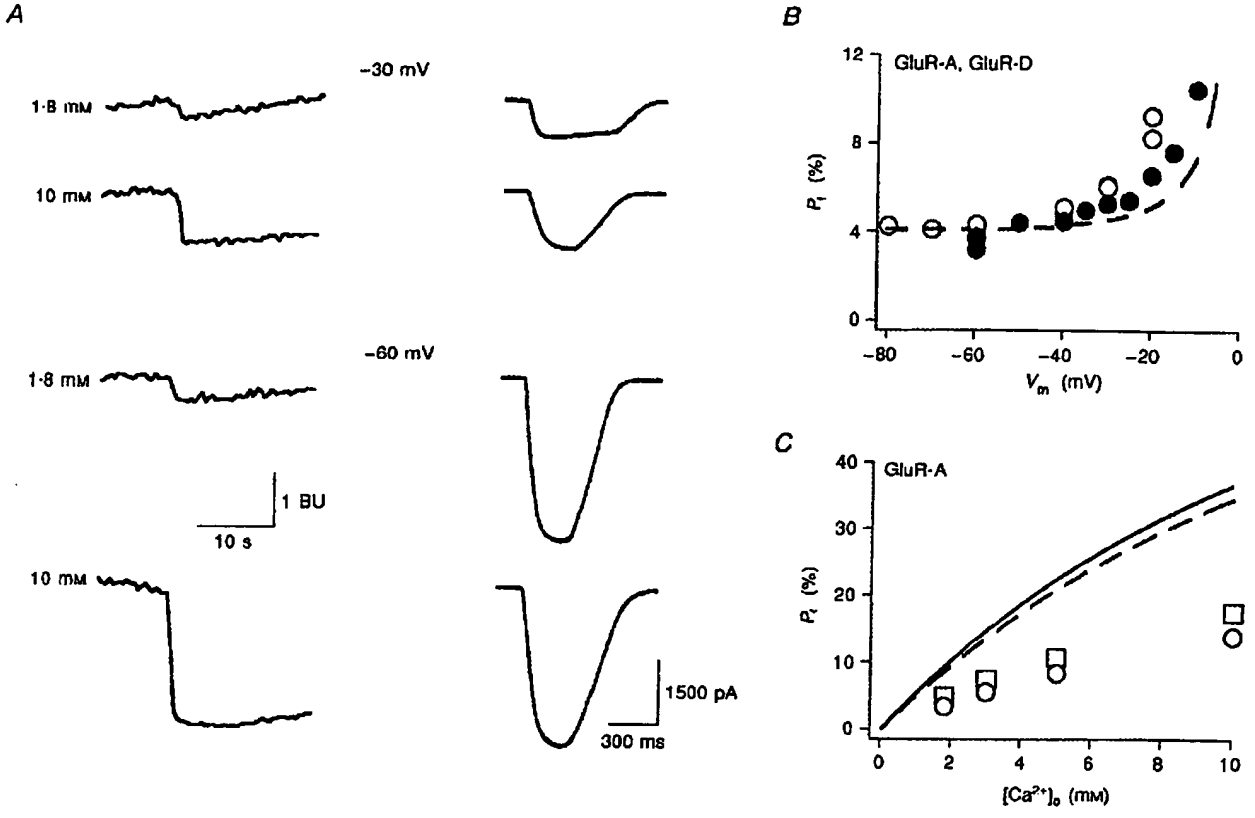

Figure 6. Fractional Ca^{2+} current through homomeric AMPAR channels

A, fluorescence decrement (ΔF_{380}) evoked by activation of GluR-A subunit channels is dependent on membrane potential and $[Ca^{2+}]_o$. Left column shows fluorescence traces at two different membrane potentials and two different $[Ca^{2+}]_o$. The corresponding glutamate-evoked whole-cell currents are shown in right column. Note that total charge transported is of approximately the same magnitude for 1·8 and 10 mM $[Ca^{2+}]_o$ (862 and 611 pA s at −30 mV; 1602 and 1641 pA s at −60 mV, respectively). At −30 mV, an increase in $[Ca^{2+}]_o$ also increases the amplitude of the whole-cell current. At −60 mV, the increase in $[Ca^{2+}]_o$ slightly decreases the current amplitude. *B*, voltage dependence of fractional Ca^{2+} current (P_f) mediated by homomeric AMPARs in 1·8 mM $[Ca^{2+}]_o$ for channels assembled from GluR-A (●) or GluR-D (○) subunits. Dashed line represents P_f–V_m relation for GluR-D subunit channels predicted by constant field assumptions using eqn (1) and setting P_f at −60 mV as a cross-point. Note the deviation of experimental values from the theoretical curve at potentials more positive than −40 mV. *C*, $[Ca^{2+}]_o$ dependence of P_f mediated by GluR-A channels at −30 (□) and −60 mV (○). Continuous and dashed lines represent theoretical curves for P_f–$[Ca^{2+}]_o$ relations at −30 and −60 mV, respectively, estimated on the basis of constant field assumptions (Methods).

Heteromeric channels assembled from Q- and R-form subunits

In some neurons native AMPAR channels are characterized by a relatively low Ca^{2+} permeability, with bi-ionic (Ca^{2+}–Cs^{+}) reversal potentials between −45 and −56 mV (Jonas & Sakmann, 1992; Jonas, Racca, Sakmann, Seeburg & Monyer, 1994) whereas in other neurons V_{rev} is close to 0 mV or positive (Jonas *et al.* 1994; Koh, Geiger, Jonas & Sakmann, 1995). The lower relative Ca^{2+} permeability of these native AMPAR channels is probably due to channel assembly from different subunits including the GluR-B(R) subunit (Burnashev *et al.* 1992*a*; Jonas *et al.* 1994). We therefore investigated Ca^{2+} influx and P_fs in cells co-transfected with cDNAs encoding the GluR-A and GluR-B(R) subunits. Experiments were performed on cells with high expression of channels, as judged by the large whole-cell current responses (1 nA or larger) to 300 μM glutamate in the presence of 10 μM cyclothiazide. Since the heteromeric AMPAR channels vary in their functional properties between cells of the same transfection, only P_f values of cells that showed a linear I–V relation in normal extracellular solution (the ratio of chord conductance at 60 and −60 mV was unity) were analysed.

Figure 7*A* illustrates the voltage dependence of ΔF_{360} in a cell transfected with equal concentrations of cDNAs encoding GluR-A and GluR-B(R) subunits. Fluorescence changes could be measured in the voltage range between 20 and −60 mV where an almost linear voltage dependence was observed. The P_f at −60 mV in cells co-transfected with GluR-A and GluR-B(R) subunit cDNAs was low (0·6%, Fig. 7*B*) and no significant voltage dependence of P_f was detectable over this limited range of potentials.

Effect of mRNA editing on fractional Ca^{2+} currents through AMPARs

Cells transfected with different ratios of cDNAs encoding R- and Q-forms of GluR-B subunits are characterized by bi-ionic reversal potentials around 0 mV suggesting that the degree of editing of the mRNA encoding the GluR-B subunit determines the relative Ca^{2+} permeability of heteromeric AMPARs (Burnashev *et al.* 1992*a*). To determine how editing controls Ca^{2+} inflow through AMPARs, we compared P_fs in cells transfected with vectors carrying only the cDNAs of the GluR-B(Q) subunit version with cells co-transfected with cDNAs encoding GluR-B(Q) and GluR-B(R) at concentration ratios of 10 : 1 or 1 : 1 (weight per volume ratios).

Figure 8*A* illustrates that P_fs at −60 mV membrane potential in cells expressing only GluR-B(Q) are relatively high (3·4%), as for GluR-A and GluR-D (Fig. 6), and the whole-cell I–V is doubly rectifying. In the cell transfected with a (10 : 1) mixture of cDNAs encoding Q- and R-forms

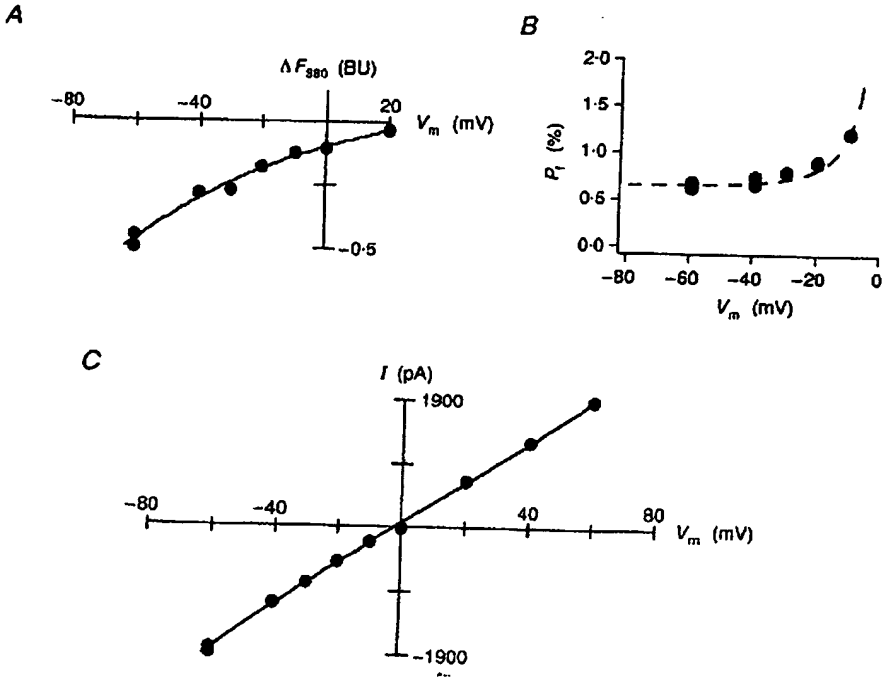

Figure 7. Fractional Ca^{2+} current through heteromeric AMPAR channels

A, voltage dependence of fluorescence decrement (ΔF_{360}) in cell co-expressing GluR-A and GluR-B(R) subunits. *B*, voltage dependence of fractional Ca^{2+} current (P_f) in cell co-expressing GluR-A and GluR-B(R) subunits. Dashed line indicates voltage dependence of P_f expected from the constant field current equation by setting the P_f value at −60 mV as cross-point. $[Ca^{2+}]_o$ is 1·8 mM. *C*, whole-cell current–voltage relation of glutamate-activated currents in the same cell as illustrated in *A* and *B*. Ratio of chord conductances at 60 and −60 mV is unity.

P_f is lower (2·9%), indicating that the relative abundance of GluR-B(R) subunit-specific mRNA determines P_f. Figure 8*B* shows also that AMPAR channels with an almost linear I–V relation (at negative membrane potentials) may mediate relatively large P_fs and have a relatively high Ca^{2+} permeability (Burnashev *et al.* 1992*a*). Finally in the cell transfected with a 1 : 1 mixture, P_f is lower, about 1% (Fig. 8*C*). No voltage dependence of the P_f was observed.

Calcium influx through KAR channel subtypes

The relative Ca^{2+} permeability (P_{Ca}/P_{Cs}) of homomeric channels formed from GluR-6 subunits of the KAR family depends on the degree of editing of mRNA at specific positions which encode amino acids of the putative transmembrane regions TM1 and TM2 (Köhler *et al.* 1993; Egebjerg & Heinemann, 1993). To find out whether differences in relative Ca^{2+} permeability (Köhler *et al.* 1993) are also seen in P_fs, we characterized those channel subtypes that may occur most frequently, based on the most abundant forms of GluR-6 mRNAs found in the CNS (Köhler *et al.* 1993). Since the current response to glutamate and kainate is rapidly desensitizing, we applied domoic acid (DA) to measure total currents (I_{KAR}) and P_fs. Alternatively, cells were pre-incubated with 0·3 mg ml^{-1} ConA (see Methods) before glutamate was applied to prevent desensitization.

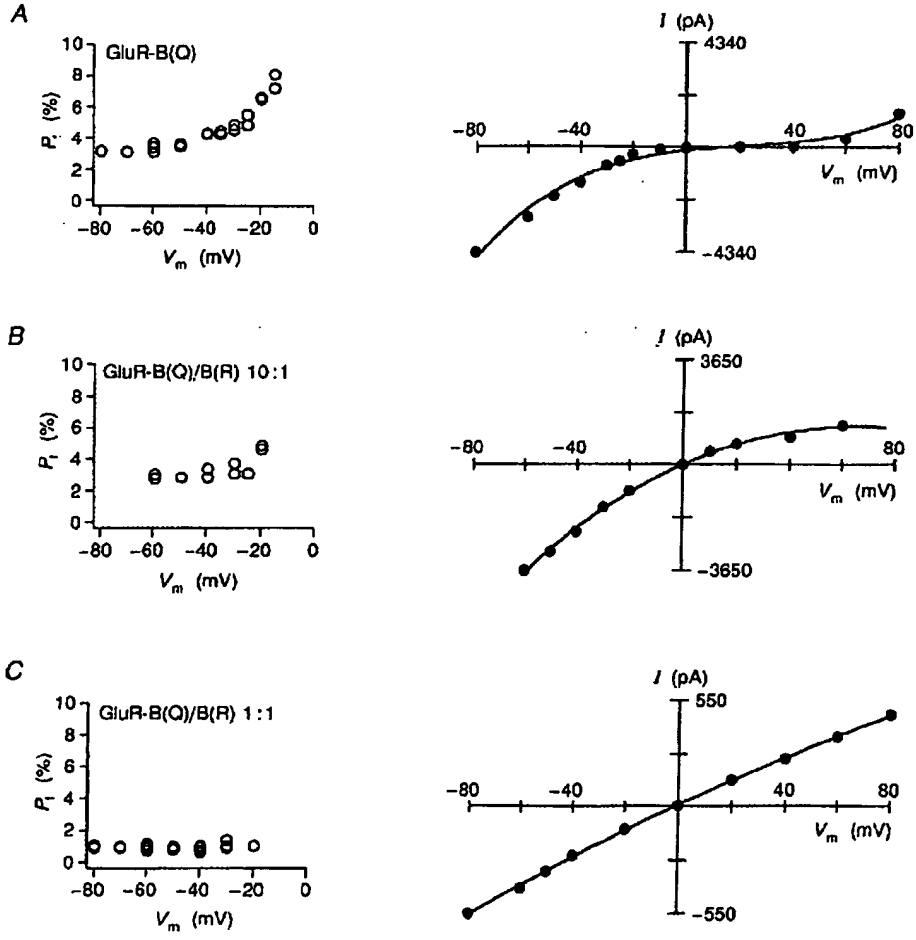

Figure 8. Fractional Ca^{2+} current through heteromeric AMPAR channels comprising Q- and R-form subunits

A, fractional Ca^{2+} current (P_f) at different membrane potentials (P_f–V_m relation, left) of a cell expressing only GluR-B(Q) subunits. Voltage dependence of whole-cell currents measured in the same cell (I–V_m relation, right). Note doubly rectifying shape of I–V_m relation. *B*, P_f–V_m (left) and I–V_m (right) relations of a cell co-expressing GluR-B(Q) and GluR-B(R) subunits. Transfection of the cell with vectors carrying cDNAs encoding Q- and R-form subunits at 10 : 1 concentration ratio. Note reduction in I–V_m rectification. Ratio of chord conductances at 60 and −60 mV is 0·4. *C*, P_f–V_m (left) and I–V_m (right) relations of a cell co-expressing GluR-B(Q) and GluR-B(R) subunits. Transfection of cell with vectors carrying cDNAs encoding Q- and R-form subunits at 1 : 1 concentration ratio. Note almost linear I–V_m relation. Chord conductances ratio is 0·85.

Effects of editing on homomeric KAR channels

Fractional Ca^{2+} currents determined for the homomeric channels formed from GluR-6 subunits in the two TM2 forms (Q- and R-form) unexpectedly had very different P_f values. Cells expressing channels assembled from R-form subunits both unedited and fully edited in TM1 showed barely detectable ΔF_{380} signals in physiological extracellular solution containing Ca^{2+} at concentrations ranging from 1·8 to up to 10 mM, although a large I_{KAR} was recorded. An upper limit of P_f that would be detectable in our experiments is 0·2%. However, ΔF_{380} signals and inward currents were measured in bi-ionic (Ca^{2+}–Cs^+) conditions. On the other hand, the P_fs through GluR-6 channels assembled from Q-form subunits in physiological external solution at −60 mV were 1·55 ± 0·15% ($n = 5$) for TM1-edited subunits and 2·0 ± 0·18% ($n = 4$) for TM1-unedited subunits, significantly lower than the value for homomeric (Q-form) AMPAR channels. The difference in P_f values for the Q-form subunits edited and unedited in TM1 indicates that editing in the TM1 region also affects P_fs through GluR-6 subunit channels. In cells co-transfected with the TM2 unedited and edited form of GluR-6 subunits the bi-ionic (Ca^{2+}–Cs^+) reversal potential was more negative than that of either of the homomeric channels (Köhler *et al.* 1993). The P_f value of the KAR channels composed of the most abundant TM1-edited Q- and R-forms of the GluR-6 subunit was 0·58 ± 0·09% ($n = 5$), intermediate between that of the corresponding homomeric R- and Q-form channels, and comparable to that of AMPAR channels formed from GluR-A and GluR-B(R) subunits.

DISCUSSION

The purpose of the experiments reported was to obtain quantitative results on P_fs mediated by different subtypes of recombinant GluR channels under clearly defined conditions of cellular fluorescence (i.e. round cells without dendrites) and with GluR-channels of known subunit composition. On the one hand the results reported allow the estimation of the contribution of different GluR subtypes to the glutamate-evoked Ca^{2+} inflow in neurones of the CNS as well as the contribution of particular subunits. On the other hand, knowledge of both P_fs and bi-ionic (Ca^{2+}–Cs^+) reversal potentials of GluR channels assembled from wild type subunits is a prerequisite for the identification of molecular determinants of Ca^{2+} influx by mutational analysis. Fractional Ca^{2+} currents mediated by recombinant GluRs vary over a more than 50-fold range, depending on

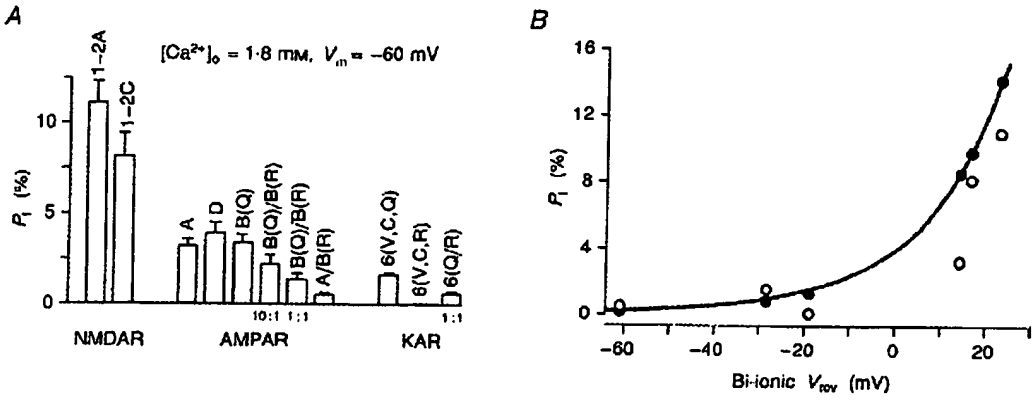

Figure 9. Fractional Ca^{2+} currents measured for different GluR channel subtypes and comparison with P_f values calculated from bi-ionic (Ca^{2+}–Cs^+) reversal potentials

A, mean values (± S.D.) of fractional Ca^{2+} currents (P_f) measured at −60 mV membrane potential in 1·8 mM $[Ca^{2+}]_o$ solution for HEK 293 cells expressing either single subunits or different combinations of subunits as indicated above each bar. P_f values (%) for NMDAR channels were: NR1–NR2A, 11·04 ± 1·25 ($n = 22$); NR1–NR2C, 8·2 ± 1·26 ($n = 20$). The values for AMPAR channels were: GluR-A, 3·2 ± 0·4 ($n = 17$); GluR-D, 3·9 ± 0·6 ($n = 6$); GluR-B(Q), 3·4 ± 0·4 ($n = 3$); GluR-B(Q)/B(R), 10 : 1, 2·2 ± 0·5 ($n = 3$); GluR-B(Q)/B(R), 1 : 1, 1·4 ± 0·3 ($n = 3$); GluR-A/B(R), 0·54 ± 0·09 ($n = 3$). For KAR channels the values were: GluR-6 (V, C, Q), 1·55 ± 0·15 ($n = 5$); GluR-6 (V, C, R), < 0·2 ($n = 16$); GluR-6(Q/R), 0·58 ± 0·09 ($n = 5$); GluR-6 (I, Y, R), < 0·2 ($n = 3$); GluR-6 (I, Y, Q), 2·0 ± 0·18 ($n = 4$). P_f values for GluR-6 subunits unedited in the TM1 region are not shown in the plot. *B*, P_f values measured in physiological extracellular solution *versus* bi-ionic V_{rev} values measured in high $[Ca^{2+}]_o$ (102 mM) bi-ionic (Ca^{2+}–Cs^+) conditions for different GluR channel subtypes (○; Table 1). P_f values calculated from the constant field current equation (●) are shown for comparison. The line represents the GHK prediction for the P_f–V_{rev} relation for V_{rev} between −60 and 30 mV under our experimental conditions. Bi-ionic V_{rev} measurements with heteromeric GluR-A/B(R) channels were made with cells which showed a linear I–V relation in normal extracellular solution, comparable to that in cells used for P_f measurements.

Table 1. Bi-ionic V_{rev} values for different GluR channel subtypes expressed in HEK cells, calculated and measured P_f values and permeability ratios P_{Ca}/P_{Cs} for high and low $[Ca^{2+}]_o$

Subunit combination	V_{rev} (mV)	P_f (%), −60 mV		P_{Ca}/P_{Cs}‡ (102 Ca^{2+}/ 143·5 Cs^+)	P_{Ca}/P_{Cs}§ (1·8 Ca^{2+}/ 143·5 Cs^+)
		Calculated †	Measured		
NR1–NR2A	22·8 ± 1·9 (n = 10)*	14·2	11·04 ± 1·25 (n = 22)	4·12	3·10
NR1–NR2C	16·5 ± 0·6 (n = 6)*	9·8	8·2 ± 1·26 (n = 20)	2·72	2·23
GluR-A	14·2 ± 0·6 (n = 4)	8·6	3·2 ± 0·4 (n = 17)	2·34	0·82
GluR-A/B(R)	−61·8 ± 1·9 (n = 4)	0·19	0·54 ± 0·09 (n = 3)	0·05	0·14
GluR-6 (V, C, R)	−19·0 ± 1·6 (n = 5)**	1·3	< 0·2 (n = 16)	0·34	< 0·05
GluR-6 (V, C, Q)	−28·4 ± 2·3 (n = 6)**	0·8	1·55 ± 0·15 (n = 5)	0·21	0·39

† P_f (%) calculated for physiological extracellular solution from GHK current eqn (1) (see Methods). ‡ P_{Ca}/P_{Cs} ratio determined for 102 mM $[Ca^{2+}]_o$ and 143·5 mM intracellular Cs^+ according to Tsno *et al.* (1990) as described in Methods (eqn (2)). The bulk concentrations were corrected for activities. § P_{Ca}/P_{Cs} ratio determined for 1·8 mM $[Ca^{2+}]_o$ (in the presence of 143·5 mM extracellular $Na^+ + K^+$) and 143·5 mM intracellular Cs^+ solution (see Methods, eqn (1)) using P_f values measured at −60 mV. The bulk concentrations were corrected for activities. * Difference in V_{rev} statistically significant (Student's t test, $\alpha > 0.01$); ** difference in V_{rev} statistically significant (Student's t test, $\alpha > 0.01$).

their composition (Fig. 9*A*). The largest P_f values are observed for heteromeric NMDAR (NR1–NR2A) channels (11%), the smallest values for homomeric KAR (GluR-6 (R)) channels (< 0·2%). Cellular mechanisms which control this remarkably wide range of P_f values are: (a) assembly of channels from different subunit families, (b) relative abundance of subunit-specific mRNAs and (c) editing of subunit mRNAs. Within each family of subunits, the AMPAR and KAR channels show a wider range of P_f values than NMDAR channels.

Fractional Ca^{2+} currents and relative Ca^{2+} permeability

Using simple models of ion permeation, it is possible to derive, from the measured P_f values, the respective P_{Ca}/P_M permeability ratios. The relation between measured P_f and the P_{Ca}/P_M for ionic conditions in our experiments ($[Ca^{2+}]_o = 1{\cdot}8$ mM and $[M^+]_i = 143{\cdot}5$ mM) assuming the validity of the Goldman–Hodgkin–Katz (GHK) equation (according to eqn (7) in Schneggenburger *et al.* 1993; but note that in the original equation the '1' is missing in $1 - \exp(2\Psi)$) is almost linear. The GHK equation rests on the assumption that there is no interaction among ions passing through the channel, an assumption which is unlikely to be true (Hille, 1992). It should therefore only be used as a starting point for a discussion of the discrepancies between measured P_f values and theoretical expectations.

Figure 9*B* shows a plot of the measured P_f values at physiological $[Ca^{2+}]_o$ (○) for different GluR channel subtypes as a function of the measured bi-ionic V_{rev} at high $[Ca^{2+}]_o$. Also included are the expected P_f values (●) calculated on the basis of bi-ionic (Ca^{2+}–Cs^+) V_{rev} measurements (Table 1).

For NMDAR channels (NR1–NR2A subtype) the bi-ionic V_{rev} of 23 mV predicts a P_f of 14%; the measured P_f is 11%, smaller than expected. Similarly, the predicted P_f value from bi-ionic V_{rev} (17 mV) for the NR1–NR2C subunit combination is 10%, but the experimentally observed value is only 8%. A somewhat larger difference between expected (from bi-ionic V_{rev} values) and measured P_f values is observed for the Ca^{2+}-permeable homomeric AMPAR channels assembled from GluR-A subunits. The bi-ionic V_{rev} is close to 14 mV predicting a P_f of 9%, the measured P_f being close to 3%. For heteromeric AMPAR channels which include an R-form subunit, the bi-ionic V_{rev} predicts a P_f of 0·2%, smaller than that measured in physiological solution (0·54%).

The discrepancy between the P_{Ca}/P_M ratios derived from P_f on the one hand and bi-ionic V_{rev} values on the other indicates that for some AMPAR, NMDAR and KAR channels constant field assumptions do not hold. Several reasons may account for this. Firstly, a larger surface potential on the internal (or external) membrane face may account for the smaller (or larger) measured P_f. Secondly, GluR channels may have saturable ion binding sites and Na^+ and Ca^{2+} may compete for them. For homomeric GluR-D channels, the P_f is voltage dependent and increases from 4% at −60 mV to up to 9% at −20 mV while constant field assumptions predict an increase to only 4·8%. The voltage dependence may indicate a voltage-dependent channel block by Ca^{2+}. Consistent with this view, it has been found that Ca^{2+} acts at low concentration as a voltage-dependent blocker of Na^+ current at potentials more negative than −30 mV (Burnashev *et al.* 1992*a*). Thirdly, heteromeric AMPARs may assemble into a mosaic of channels with different subunit composition and inclusion

of GluR-B(R) subunits could change Ca^{2+} permeability more than it affects Ca^{2+} conductance.

Fractional Ca^{2+} currents determined for GluR-6 channel subtypes show the largest discrepancy between expected (from bi-ionic V_{rev}, Table 1) and measured P_f values. Ca^{2+} inflow is largest for the TM2 Q-form and smallest for the R-form of GluR-6 channels regardless of TM1 editing. Therefore, mRNA editing in the TM2 segment regulates Ca^{2+} inflow through KAR channels in a way similar to that of AMPARs; by editing GluR-6 mRNA in the triplet which encodes the amino acid at the Q/R site, the Ca^{2+} inflow is almost abolished. This result is the opposite to what one may expect on the basis of V_{rev} measurements (Table 1, Köhler *et al.* 1993). Unexpectedly reduced P_f values for the R-form of GluR-6 channels might be, at least partly, explained by a strong interaction of the Ca^{2+} and Na^+ ions. For example, despite the higher Ca^{2+} permeability estimated from the bi-ionic reversal potentials, the Ca^{2+} conductance of the GluR-6R channels in the presence of Na^+ ions might be much smaller than that in pure Ca^{2+} solution.

Relation between recombinant and native GluR channels

In stellate cells of the visual cortex the P_{Ca}/P_M permeability ratio of AMPAR channels (bi-ionic V_{rev} is close to 0 mV) is higher than that of pyramidal cells (bi-ionic V_{rev} more negative than −50 mV) (Jonas *et al.* 1994). This difference in relative Ca^{2+} permeability was traced to the lower abundance of GluR-B(R)-specific mRNA (Jonas *et al.* 1994). This is in agreement with the finding that a lower concentration of GluR-B(R) cDNA, when co-transfecting HEK 293 cells with Q- and R-form cDNA-carrying vectors, generates recombinant AMPAR channels which are characterized by a P_f of 2% and a bi-ionic V_{rev} close to 0 mV (Burnashev *et al.* 1992*a*). In cells where the mRNAs encoding the Q-form subunits and those encoding GluR-B(R) subunits are presumably equal in abundance, channels are expressed which are characterized by a mean P_f of 0·54% and a bi-ionic V_{rev} close to −60 mV. The bi-ionic V_{rev} in these cells is comparable to that observed in neocortical pyramidal cells where indeed the GluR-B(R) mRNA is relatively more abundant than in stellate cells (Fig. 5 in Jonas *et al.* 1994).

It has been suggested that P_fs in septal neurones mediated by AMPAR and NMDAR channels vary only over a fivefold range (Schneggenburger *et al.* 1993). Whole-cell currents evoked by kainate and presumably mediated by AMPARs have a P_f of 1·4%, those mediated by NMDARs a P_f of 6·8%. The relatively high P_f value for AMPARs could indicate that in septal neurones these receptors are more Ca^{2+} permeable than, for example, those in hippocampal or neocortical pyramidal cells and may be comparable to those of stellate cells in neocortex or basket cells in dentate gyrus (Jonas *et al.* 1994; Koh *et al.* 1995). Alternatively, co-activation of KAR channel subtypes may have contributed significantly to the relatively high P_f values for AMPAR/KAR channels in septal neurones. Likewise, the lower P_f values (6·8%) for currents generated by NMDAR activation may reflect predominant activation of NR2C subtype or more complex subunit assembly (rather than that of the NR2A subtype). Measurement of bi-ionic (Ca^{2+}–Cs^+) reversal potentials of glutamate-activated currents in septal neurons may provide further clues to identify the GluR-subunits expressed.

For native NMDAR channels in cultured rat hippocampal cells, P_f values were calculated using constant field assumptions and, in addition, assuming a simple channel block mechanism by Ca^{2+} (Jahr & Stevens, 1993). We calculate for this channel a P_f of 13·4% for 1·8 mM $[Ca^{2+}]_o$, which is in the range of that measured directly for a recombinant NMDAR channel with a comparable bi-ionic V_{rev}.

The smaller P_f value for NR1–NR2C channels as compared with NR1–NR2A channels may be due to stronger block of P_fs by Ca^{2+}. This assumption predicts a shallower blocking curve of single-channel conductance with increasing $[Ca^{2+}]_o$ for NR1–NR2C receptors. The reduction of the whole-cell chord conductance with $[Ca^{2+}]_o$, ranging from 50 μM to 110 mM, was indeed shallower for NR1–NR2C channels as compared with NR1–NR2A channels (not shown).

Functional significance of differences in fractional Ca^{2+} currents

An interesting functional aspect of Ca^{2+} inflow through GluR channels is that in neurons which express Ca^{2+}-permeable AMPARs (Jonas *et al.* 1994; Koh *et al.* 1995) during the peak of EPSCs the Ca^{2+} inflow mediated by AMPARs and NMDARs could be comparable in size. The contribution of different GluR channel subtypes to the inflow of Ca^{2+} during EPSPs in CNS neurones may be estimated by using the relation established for V_{rev} and P_f values for various recombinant GluR channels. In stellate cells of the visual cortex the EPSC is mediated by co-activation of AMPAR and NMDAR channels and the relative amplitude of the EPSC peak current mediated by Ca^{2+}-permeant AMPA and NMDAR channels varies between 1:1 and 10:1 in different synapses (Stern, Edwards & Sakmann, 1992). If it is assumed that the P_f for the EPSC component mediated by Ca^{2+}-permeable AMPARs (Jonas *et al.* 1994) is on average 3% and the P_f of NMDARs is 10%, then in these synapses most of the Ca^{2+} inflow through the postsynaptic membrane at the peak of the EPSP would be mediated by AMPAR channels. Over longer integration times, however, Ca^{2+} inflow is dominated by NMDAR channels (see Koh *et al.* 1995).

One presumed function of NMDAR channels is to allow coincidence detection of presynaptic electrical activity by a transient increase in postsynaptic Ca^{2+} inflow (Bourne & Nicoll, 1993). In cerebellar granule cells, postnatally an increase in NR2C subunit mRNA abundance is observed (Monyer *et al.* 1994). Fractional Ca^{2+} currents are smaller for NR2C subunit-containing channels and, therefore, the altered gene expression pattern in the cerebellum may change the voltage range of coincidence detection by reducing Ca^{2+} inflow at −20 mV (because of the smaller P_f of a NR2C subunit-containing channel), but increasing Ca^{2+} inflow at −40 mV (because of the weaker Mg^{2+} block of a NR2C-containing channel). The postnatal switch in abundance of NMDAR-subunit mRNAs, therefore, could enable neurones to detect weaker coincidences.

Ascher, P. & Nowak, L. (1988). The role of divalent cations in the *N*-methyl-D-aspartate responses of mouse central neurones in culture. *Journal of Physiology* **399**, 247–266.

Bourne, H. R. & Nicoll, R. (1993). Molecular machines integrate coincident synaptic signals. *Cell* **72** */Neuron* **10** (suppl.), 65–75.

Burnashev, N., Monyer, H., Seeburg, P. H. & Sakmann, B. (1992*a*). Divalent ion permeability of AMPA receptor channels is dominated by the edited form of a single subunit. *Neuron* **8**, 189–198.

Burnashev, N., Schoepfer, R., Monyer, H., Ruppersberg, J. P., Günther, W., Seeburg, P. H. & Sakmann, B. (1992*b*). Control by asparagine residues of calcium permeability and magnesium blockade in the NMDA receptor. *Science* **257**, 1415–1419.

Collingridge, G. L. & Bliss, T. V. P. (1987). NMDA receptors – their role in long-term potentiation. *Trends in Neurosciences* **10**, 288–293.

Collingridge, G. L. & Singer, W. (1990). Excitatory amino acid receptors and synaptic plasticity. *Trends in Pharmacological Sciences* **11**, 290–296.

Egebjerg, J. & Heinemann, S. F. (1993). Ca^{2+} permeability of unedited and edited versions of the kainate-selective glutamate receptor GluR6. *Proceedings of the National Academy of Sciences of the USA* **90**, 755–759.

Grynkiewicz, G., Poenie, M. & Tsien, R. (1985). A new generation of Ca^{2+} indicators with greatly improved fluorescence properties. *Journal of Biological Chemistry* **260**, 3440–3450.

Hamill, O. P., Marty, A., Neher, E., Sakmann, B. & Sigworth, F. J. (1981). Improved patch clamp techniques for high-resolution current recording from cells and cell-free membrane patches. *Pflügers Archiv* **391**, 85–100.

Hille, B. (1992). *Ionic Channels of Excitable Membranes*. Sinauer Associates Inc., Sunderland, MA, USA.

Hollmann, M., Hartley, M. & Heinemann, S. (1991). Ca^{2+} permeability of KA–AMPA-gated glutamate receptor channels dependence on subunit composition. *Science* **252**, 851–853.

Iino, M., Ozawa, S. & Tsuzuki, K. (1990). Permeation of calcium through excitatory amino acid receptor channels in cultured rat hippocampal neurones. *Journal of Physiology* **424**, 151–165.

Jahr, C. E. & Stevens, C. F. (1993). Calcium permeability of the *N*-methyl-D-aspartate receptor channel in hippocampal neurons in culture. *Proceedings of the National Academy of Sciences of the USA* **90**, 11573–11577.

Jonas, P., Racca, C., Sakmann, B., Seeburg, P. H. & Monyer, H. (1994). Differences in Ca^{2+} permeability of AMPA-type glutamate receptor channels in neocortical neurons caused by differential GluR-B subunit expression. *Neuron* **12**, 1281–1289.

Jonas, P. & Sakmann, B. (1992). Glutamate receptor channels in isolated patches from CA1 and CA3 pyramidal cells of rat hippocampal slices. *Journal of Physiology* **455**, 143–171.

Koh, D.-S., Geiger, J. R. P., Jonas, P. & Sakmann, B. (1995). Ca^{2+}-permeable AMPA and NMDA receptor channels in basket cells of rat hippocampal dentate gyrus. *Journal of Physiology* **485**, 383–402.

Köhler, M., Burnashev, N., Sakmann, B. & Seeburg, P. H. (1993). Determinants of Ca^{2+} permeability in both TM1 and TM2 of high affinity kainate receptor channels: diversity by RNA editing. *Neuron* **10**, 491–500.

Mayer, M. L. & Westbrook, G. L. (1987). Permeation and block of *N*-methyl-D-aspartic acid receptor channels by divalent cations in mouse cultured central neurones. *Journal of Physiology* **394**, 501–527.

Mayer, M. L., Westbrook, G. L. & Guthrie, P. B. (1984). Voltage-dependent block by Mg^{2+} of NMDA responses in spinal cord neurones. *Nature* **309**, 261–263.

Monaghan, D. T., Bridges, R. J. & Cotman, C. W. (1989). The excitatory amino acid receptors: Their classes, pharmacology, and distinct properties in the function of the central nervous system. *Annual Review of Pharmacology and Toxicology* **29**, 365–402.

Monyer, H., Burnashev, N., Laurie, D. J., Sakmann, B. & Seeburg, P. H. (1994). Developmental and regional expression in the rat brain and functional properties of four NMDA receptors. *Neuron* **12**, 529–540.

Moriyoshi, K., Masu, M., Ishii, T., Shigemoto, R., Mizuno, N. & Nakanishi, S. (1991). Molecular cloning and characterization of the rat NMDA receptor. *Nature* **354**, 31–37.

Neher, E. & Augustine, G. J. (1992). Calcium gradients and buffers in bovine chromaffin cells. *Journal of Physiology* **450**, 273–301.

Nicoll, R. A., Kauer, J. A. & Malenka, R. C. (1988). The current excitement in long-term potentiation. *Neuron* **1**, 97–103.

Schneggenburger, R., Zhou, Z., Konnerth, A. & Neher, E. (1993). Fractional contribution of calcium to the cation current through glutamate receptor channels. *Neuron* **11**, 133–143.

Sommer, B., Keinänen, K., Verdoon, T. A., Wisden, W., Burnashev, N., Herb, A., Köhler, M., Takagi, T., Sakmann, B. & Seeburg, P. H. (1990). Flip and flop: A cell-specific functional switch in glutamate operated channels of the CNS. *Science* **249**, 1580–1585.

Stern, P., Edwards, F. A. & Sakmann, B. (1992). Fast and slow components of unitary EPSCs on stellate cells elicited by focal stimulation in slices of rat visual cortex. *Journal of Physiology* **449**, 247–278.

Sun, D. D., Chang, F. C., Chien, A., Zhao, X.-L., Shirokov, R., Rios, E. & Hosey, M. M. (1994). Expression of functional cardiac L-type Ca^{2+} channels in transiently transfected HEK (293) cells. *Biophysical Journal* **66**, A320.

Watkins, J. C., Krogsgaard-Larsen, P. & Honore, T. (1990). Structure–activity relationships in the development of excitatory amino acid receptor agonists and competitive antagonists. *Trends in Pharmacological Sciences* **11**, 25–33.

Wisden, W. & Seeburg, P. H. (1993). Mammalian ionotropic glutamate receptors. *Current Opinion in Neurobiology* 3, 291–298.

Zhou, Z. & Neher, E. (1993). Calcium permeability of nicotinic acetylcholine receptor channels in bovine adrenal chromaffin cells. *Pflügers Archiv* 425, 511–517.

Acknowledgements

We thank Professor P. H. Seeburg (Zentrum für Molekulare Biologie Heidelberg (ZMBH)) for providing clones of GluR subunits and Ms Grünewald (ZMBH) for cell culture and transfections. We are also grateful to A. Roth for performing the simulations and to Dr N. Spruston for critically reading the manuscript. The expert secretarial assistance of Ms Dücker and Ms Spiegel is acknowledged.

Author's present address

Z. Zhou: Renal Division, Jewish Hospital, Washington University Medical Center, St Louis, MO 63110, USA.

Received 2 September 1994; accepted 31 October 1994.